Disease Models & Mechanisms 2, 389-398 (2009) doi:10.1242/dmm.002386
Published by The Company of Biologists 2009

Rapamycin suppresses seizures and neuronal hypertrophy in a mouse model of cortical dysplasia

M. Cecilia Ljungberg[1,2,*], C. Nicole Sunnen[1,3,*], Joaquin N. Lugo[1,2], Anne E. Anderson[1,2,3] and Gabriella D'Arcangelo[4,‡]

SUMMARY

Malformations of the cerebral cortex known as cortical dysplasia account for the majority of cases of intractable childhood epilepsy. With the exception of the tuberous sclerosis complex, the molecular basis of most types of cortical dysplasia is completely unknown. Currently, there are no good animal models available that recapitulate key features of the disease, such as structural cortical abnormalities and seizures, hindering progress in understanding and treating cortical dysplasia. At the neuroanatomical level, cortical abnormalities may include dyslamination and the presence of abnormal cell types, such as enlarged and misoriented neurons and neuroglial cells. Recent studies in resected human brain tissue suggested that a misregulation of the PI3K (phosphoinositide 3-kinase)-Akt-mTOR (mammalian target of rapamycin) signaling pathway might be responsible for the excessive growth of dysplastic cells in this disease. Here, we characterize neuronal subset (NS)-*Pten* mutant mice as an animal model of cortical dysplasia. In these mice, the *Pten* gene, which encodes a suppressor of the PI3K pathway, was selectively disrupted in a subset of neurons by using Cre-*loxP* technology. Our data indicate that these mutant mice, like cortical dysplasia patients, exhibit enlarged cortical neurons with increased mTOR activity, and abnormal electroencephalographic activity with spontaneous seizures. We also demonstrate that a short-term treatment with the mTOR inhibitor rapamycin strongly suppresses the severity and the duration of the seizure activity. These findings support the possibility that this drug may be developed as a novel antiepileptic treatment for patients with cortical dysplasia and similar disorders.

INTRODUCTION

Cortical dysplasia is a broad category of disorders that includes focal cortical dysplasia (FCD) and hemimegalencephaly (HMEG), which are developmental abnormalities of unknown etiology that are highly associated with intractable childhood epilepsy (Cepeda et al., 2006). Currently, no genetic animal models that recapitulate key traits of the disease are available to investigate molecular mechanisms and to develop new treatments.

Because of the presence of abnormal brain structures (cortical tubers), tuberous sclerosis complex (TSC) can be considered a type of cortical dysplasia (Vinters et al., 1999). TSC is a congenital disorder resulting from mutations in the *TSC1* or *TSC2* genes (European Chromosome 16 Tuberous Sclerosis Consortium, 1993; van Slegtenhorst et al., 1997). A prominent neurological characteristic of TSC is epilepsy, which is often present in early childhood, but other manifestations such as subependymal giant cell astrocytomas, learning disabilities and autism are also present in varying degrees of comorbidity. Despite advances in understanding the molecular defects in TSC, the mechanisms of epileptogenesis are not well understood.

Previous studies have implicated the PI3K (phosphoinositide 3-kinase)-Akt-mTOR (mammalian target of rapamycin) signaling pathway in cortical dysplasia, and demonstrated that mTOR activity is dysregulated in the enlarged neurons and neuroglial cells that are found in TSC (Baybis et al., 2004; Miyata et al., 2004), as well as in FCD and HMEG patients (Ljungberg et al., 2006). The activity of this pathway is normally controlled by the product of the tumor suppressor gene *PTEN* (phosphatase and tensin homolog on chromosome ten) and by the products of the *TSC1* (hamartin) and *TSC2* (tuberin) genes. Hamartin and tuberin are upstream suppressors of mTOR kinase. *PTEN* encodes a lipid and protein phosphatase that modulates cell growth by negatively regulating PI3K (Maehama and Dixon, 1998). The activation of PI3K results in the phosphorylation of Akt and mTOR, which in turn stimulates protein synthesis through phosphorylation of ribosomal proteins and translation factors (Harris and Lawrence, 2003). This pathway is essential for control of normal cell growth, proliferation and survival in both invertebrates and vertebrates (Leevers et al., 1999).

Inherited mutations in the human *PTEN* gene confer cancer predisposition, and sporadic loss-of-heterozygosity mutations result in a variety of cancers (Li et al., 1997; Chow and Baker, 2006). Germline mutations of the *PTEN* gene also produce distinct clinical syndromes with variable neurological manifestations (Eng, 2003). In the mouse, heterozygous *Pten* deletions resulted in the formation of tumors in multiple organs (Suzuki et al., 1998; Podsypanina et al., 1999). Brain neuron-specific *Pten* deletions resulted in ataxia, seizures and macrocephaly, which were associated with the phosphorylation of Akt and mTOR in mutant neurons (Backman et al., 2001; Kwon et al., 2001; Kwon et al., 2006).

In this study, we focused on mTOR activation as a common mechanism of disease that is altered in several types of cortical dysplasia, and characterized mutant mice in which the *Pten* gene is selectively deleted in a subset of neurons (NS-*Pten* mutants). We report that these mutants display molecular, cellular and physiological traits of cortical dysplasia that can be effectively suppressed by a short-term treatment with the mTOR inhibitor rapamycin.

[1]The Cain Foundation Laboratories, Texas Children's Hospital, [2]Department of Pediatrics and [3]Department of Neuroscience, Baylor College of Medicine, Houston, TX 77030, USA
[4]Department of Cell Biology and Neuroscience, Rutgers, The State University of New Jersey, Piscataway, NJ 08854, USA
*These authors contributed equally to this work
‡Author for correspondence (e-mail: darcangelo@biology.rutgers.edu)

RESULTS

Pten is deleted in a subset of cortical neurons in NS-*Pten* mutants

We examined the brain anatomy and the cortical loss of Pten protein expression in homozygous mutants compared with their wild-type littermates. The mutant mice were described previously as $Pten^{loxP/loxP}$; *Gfap-Cre* mice (Backman et al., 2001; Kwon et al., 2001) and were reported to exhibit *Pten* deletion in a subset of neuronal cells, including the majority of granule cells in the dentate gyrus and cerebellum. To distinguish this mouse line from other lines where the *Gfap* promoter drives Cre expression and *Pten* deletion in astrocytes (Fraser et al., 2004), we refer to it here as neuronal subset-specific *Pten* (NS-*Pten*). Consistent with previous reports, we found that NS-*Pten* heterozygous mice appear normal, whereas homozygous mutants display ataxia and premature mortality. At the neuroanatomical level, mutants displayed macrocephaly, with apparent enlargement of cortical, hippocampal and cerebellar structures (Fig. 1A). The extent of the enlargement varied somewhat among individual mutants, but it was most readily and consistently observed in the hippocampus, a structure that also appeared mildly dysmorphic. The hippocampal and cerebellar abnormalities correlated strongly with loss of *Pten* gene expression in the majority of neurons in these structures (not shown), as reported previously (Backman et al., 2001; Kwon et al., 2001).

When the neocortex of mutant mice was examined in detail by immunofluorescence, loss of Pten protein expression was noted in many cortical neurons in all cellular layers (Fig. 1B). Mutant neurons, identified by the expression of the neuronal marker NeuN, appeared enlarged compared with adjacent Pten-positive neurons,

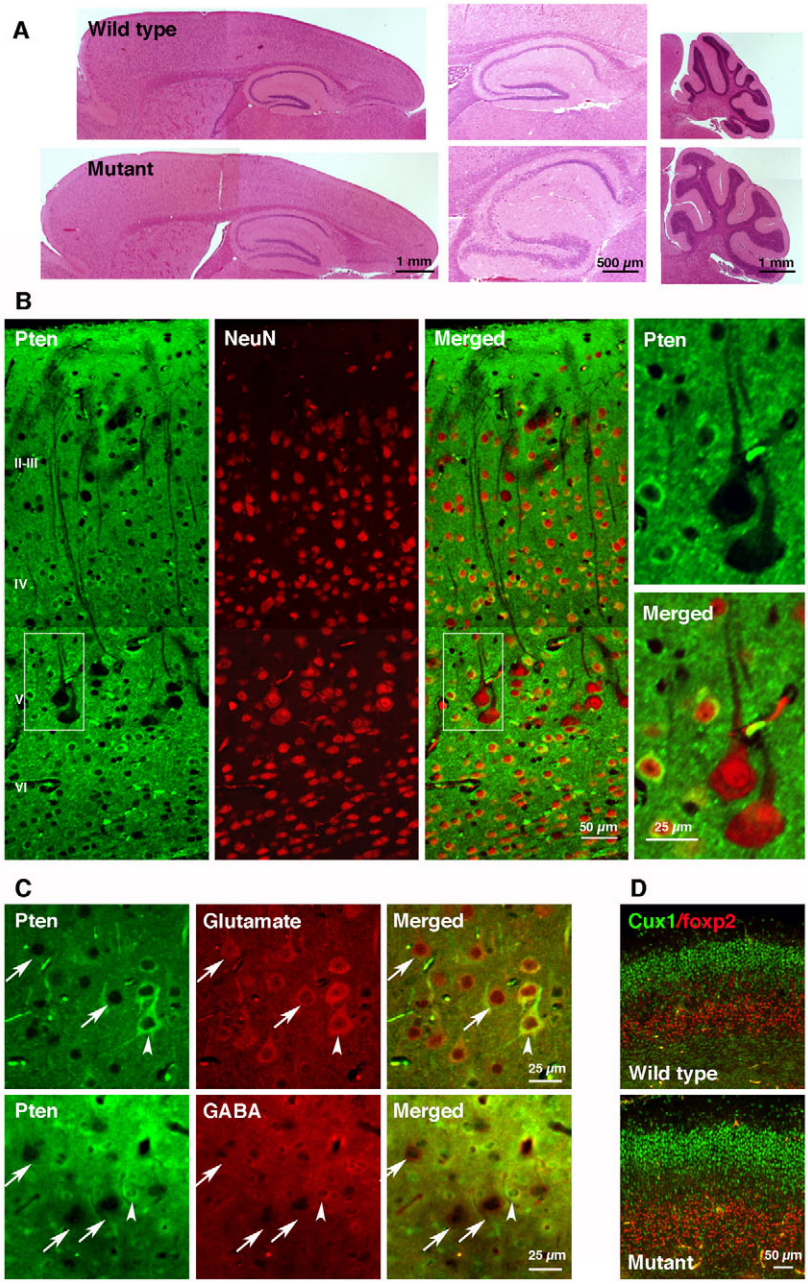

Fig. 1. Macrocephaly and Pten loss in the neocortex of NS-*Pten* mutant mice. (A) Hematoxylin and eosin (H&E) staining of sagittal brain sections derived from wild-type and NS-*Pten* mutant mice. The mutant brain is enlarged compared with the wild-type brain. The cerebral cortex (left panels) is affected mildly, whereas both the hippocampus (middle panels) and cerebellum (right panels) display obvious enlargement and structural abnormalities. (B) Pten (green) and NeuN (red) double immunofluorescence on paraffin-embedded sagittal sections (close to the midline) of the NS-*Pten* mutant cortex. The smaller panels on the right represent enlargements of the boxed areas in the Pten-stained and merged images. Many large pyramidal-shaped neurons in layer V and some neurons in other cortical layers are Pten negative. (C) The top panels show a section of NS-*Pten* mutant neocortex that has been double labeled with Pten (green) and glutamate (red) antibodies. The lower panels show double immunofluorescence with Pten (green) and GABA (red) antibodies. Pten-negative neurons (arrows) always express glutamate but not GABA, whereas the large Pten-positive neurons (arrowheads) express glutamate and the small Pten-positive neurons (arrowheads) express GABA. (D) Double labeling of cortical sections derived from E18.5 wild-type or NS-*Pten* mutant mice with antibodies against Cux1 (green, layer II-IV) and foxp2 (red, layer VI). The cortical layers appear normal in the mutant mice.

but retained proper orientation and morphology that are typical of their layer. For example, mutant neurons in layer V displayed a prominent apical dendrite, oriented radially towards the top of the cortex (Fig. 1B). This morphology is typical of large pyramidal neurons, which are excitatory, early-born principal neurons that originate in the ventricular zone of the neocortex. To determine whether Pten-negative neurons also retained their neurochemical characteristics, we conducted double immunolabeling with antibodies against Pten and either glutamate, a marker of excitatory neurons, or γ-aminobutyric acid (GABA), a marker of inhibitory neurons. We found that virtually all Pten-negative neurons were glutamatergic (Fig. 1C, top panels), whereas none were GABAergic (Fig. 1C, lower panels). Finally, we sought to determine whether loss of Pten results in abnormal radial migration and positioning of mutant neurons into cortical layers. Brain sections obtained from wild-type and homozygous NS-*Pten* mutant mice at embryonic day (E)18.5 were double labeled with antibodies against Cux1, a marker of upper cortical layers, and foxp2, a marker of deep cortical layers (Fig. 1D). These markers labeled the appropriate cellular layers in wild-type and mutant cortex, indicating that Pten loss does not affect neuronal migration.

Together, our findings that neuronal morphology, neurotransmitter and layer-specific marker expression are not altered in NS-*Pten* mutant mice indicate that Pten loss in cortical neurons does not disrupt their cell-specific phenotype.

Cortical neurons lacking Pten are hypertrophic

Despite their overall normal phenotype, Pten mutant cortical neurons appeared enlarged compared with adjacent normal cells. To examine the size of mutant cortical neurons in more detail, we performed immunohistochemistry with Pten antibodies, and used hematoxylin counterstaining to distinguish and outline the cell bodies of Pten-positive and -negative neurons in the neocortex of mutant mice (Fig. 2A,B). We used a similar approach to label Pten-positive neurons in the wild-type neocortex. Because the cell body size of cortical neurons varies greatly depending on the cellular layer where they reside, we limited our analysis to neurons located in layer V. This layer was chosen because it contained a large number of Pten-negative, as well as Pten-positive, pyramidal neurons that could be identified easily owing to their relatively large size. We then measured the cell body size of positive and negative neurons in layer V of the cortex in mutant mice, and the cell body size of positive layer V pyramidal neurons in wild-type animals. At postnatal day (P)12 there was a significant difference (~1.7-fold increase) in the soma size of neurons lacking Pten (393.1±10.8 μm^2) compared with that of Pten-expressing neurons in both NS-*Pten* mutant (213.8±28 μm^2) and wild-type (227.6±30.6 μm^2) animals (Fig. 2C). Similar results were obtained when adult mice (9 weeks of age) were analyzed. The soma size of Pten-deficient neurons was significantly increased (381.9±22.4 μm^2) compared with that of Pten-positive neurons in the cortex from either mutant (234.9±15.9 μm^2) or wild-type mice (225.1±10.8 μm^2) (Fig. 2C). Thus, unlike the Pten-negative hippocampal and cerebellar granule neurons that were measured in previous studies (Backman et al., 2001; Kwon et al., 2001), the size of Pten-negative cortical pyramidal neurons did not increase progressively with age after the second postnatal week. There was no significant difference in soma size between the Pten-positive cells in mutant and wild-type mice at any age analyzed (Fig. 2C).

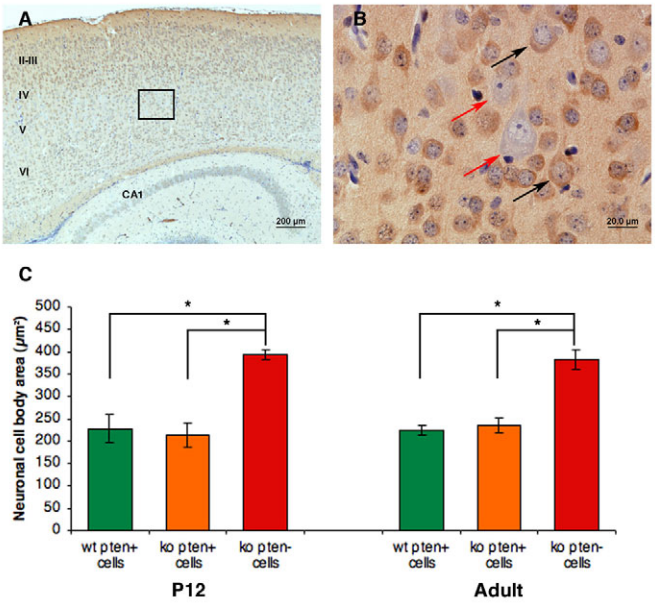

Fig. 2. Cortical neurons lacking Pten are hypertrophic. Pten-positive and -negative cortical neurons were visualized by immunohistochemistry and hematoxylin counterstaining. (A) Sagittal section taken through the neocortex of a NS-*Pten* mutant mouse, illustrating the distribution of both Pten-positive (brown) and -negative cells. (B) Layer V neurons that lack Pten staining (red arrows) appear larger than adjacent Pten-positive neurons (black arrows) in the cortex of NS-*Pten* mutant mice. (C) Quantitative analysis of the cell body size of Pten-negative and -positive neurons in cortical layer V of mutant mice, and of the corresponding Pten-positive neurons in wild-type mice, at the indicated ages (n=3 for each age and genotype) is shown. Pten-negative neurons are significantly larger than Pten-positive neurons from either mutant or wild-type animals [*P<0.01 by analysis of variance (ANOVA) with Tukey's honestly significant difference (HSD) test]. Data is shown as the mean cell body area ± s.e.m.

Increased activation of the mTOR pathway in Pten-deficient cells

Pten is a negative regulator of the PI3K pathway and its loss causes increased activation of the downstream Akt and mTOR kinases (Backman et al., 2002). We investigated the activity of the PI3K pathway by immunohistochemistry and immunofluorescence using phospho-specific antibodies directed against Akt (Ser473) and downstream targets of mTOR, such as the translation initiation factor eIF4G (Ser1108) and the ribosomal protein S6 (Ser240/244) (Sarbassov et al., 2005). We have shown previously that the phosphorylation level of these proteins is increased in cytomegalic neurons in human cortical dysplasia (Ljungberg et al., 2006). Our present data revealed an increase in phosphorylated Akt, eIF4G and ribosomal protein S6 in NS-*Pten* mutant animals (Fig. 3A). Consistent with earlier reports, the phospho-Akt signal was particularly strong in the dentate gyrus and the hippocampus (Kwon et al., 2001), but it was also seen in the neocortex of NS-*Pten* mutant mice. The phospho-eIF4G signal was weak in the normal brain but it appeared elevated in the dentate gyrus, the CA1 region of the hippocampus, and layer V of the neocortex in the NS-*Pten* mutant brain. The phospho-S6 signal, was generally strong in the forebrain of both wild-type and mutant animals, and it appeared to be increased in the cortical and hippocampal structures of NS-*Pten* mutant mice.

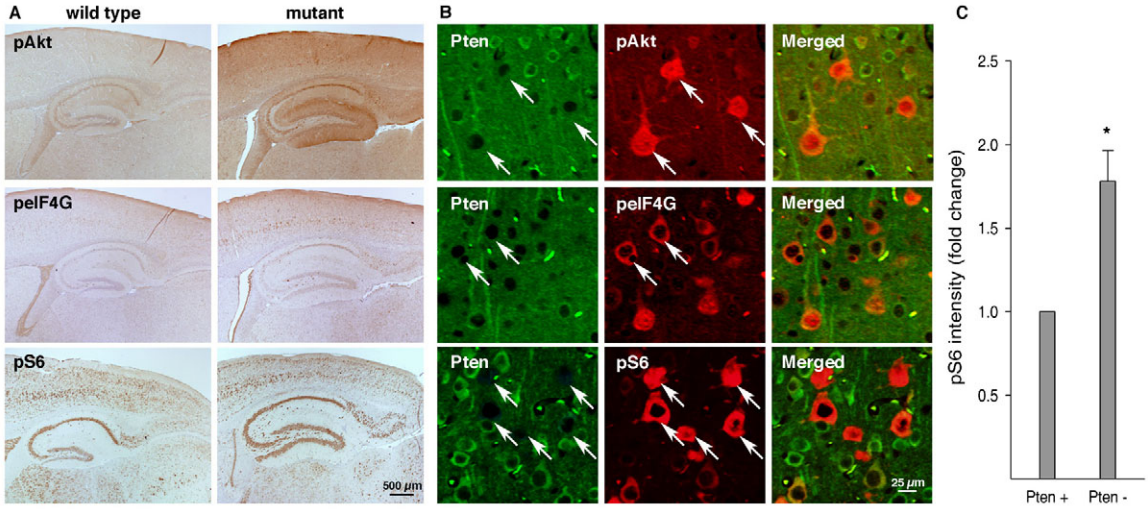

Fig. 3. The Akt-mTOR pathway is activated in the neocortex of NS-*Pten* mutant mice. (A) Sections of adult wild-type and mutant mice were processed for immunohistochemistry using antibodies against phospho-Akt (pAkt), phospho-eIF4G (pelF4G) and phospho-S6 (pS6). Elevated levels of these phosphoproteins can be seen in the neocortex and hippocampus of mutant animals. (B) Higher magnification images of cortical layer V from a mutant mouse section that has been double labeled by immunofluorescence show that many Pten-negative cells (arrows in green images) also exhibit elevated levels of pAkt, pelF4G or pS6 (arrows in all red images). (C) Quantification of the pS6 fluorescence signal in Pten-negative and -positive layer V neurons shows that the levels of S6 phosphorylation are statistically increased in mutant neurons compared with normal neurons in 9-week-old mutant mice (n=3, *P<0.05).

To look in more detail at the activation of the PI3K pathway in the mutant neocortex, we performed double immunofluorescence using Pten and phospho-specific antibodies targeting the Akt-mTOR pathway (Fig. 3B). The majority of the Pten-negative neurons in the layer V cortex displayed strong phospho-Akt, phospho-eIF4G and phospho-S6 immunoreactivity in both the cytoplasm and the nucleus. Some Pten-positive cortical neurons were also positive for phospho-eIF4G and phospho-S6, although, overall, the mutant neurons displayed stronger staining. Quantitative analysis confirmed that the phospho-S6 immunofluorescence was significantly increased in mutant neurons compared with Pten-positive neurons in NS-*Pten* mice (Fig. 3C). These data demonstrate that the PI3K-Akt-mTOR pathway is overactive in mutant Pten-deficient cortical neurons.

NS-*Pten* mutant mice exhibit spontaneous seizures and abnormal electroencephalogram (EEG) activity

Previous studies with NS-*Pten* mutants indicated that these mice have spontaneous seizures, characterized by forelimb clonus and tonic-clonic events (Backman et al., 2001; Kwon et al., 2001). We also observed tonic-clonic seizures in some of the mutant mice as they aged beyond 6 weeks. To examine the seizure phenotype in more detail, and to determine whether NS-*Pten* mutants have subclinical epileptiform activity that does not manifest in overt behavioral seizures, we conducted synchronized video-EEG recordings. Animals were implanted with cortical electrodes during postnatal week 3, and monitored for an average of 4.91 hours per week from postnatal week 4 to 9. By 6 weeks of age, all NS-*Pten* mutant mice (n=7) displayed subclinical electrographic seizures lasting for at least 10 seconds (Table 1), even though most of these mice (n=5/7) lacked any obvious behavioral correlate. However, at this age, two of the seven mice also exhibited behavioral changes that were characterized by tonic-clonic activity and, by 9 weeks of age, three of the seven mice exhibited these types of seizures. Moreover, we detected a number of different types of abnormal epileptiform activity, as well as abnormalities in the awake baseline EEG activity that were never seen in wild-type animals (n=6) (Table 1). In addition to subclinical seizures, mutant animals also exhibited isolated interictal spikes, short trains of

Table 1. Number of animals exhibiting each type of epileptiform activity at 6 and 9 weeks of age

Genotype	Treatment	Age (wks)	*n*	Spikes	Repetitive spikes (<5 seconds)	Repetitive spike runs (>5-<10 seconds)	Seizures (>10 seconds)
Wild type	Naïve	6	6	0 (0)	0 (0)	0 (0)	0 (0)
Mutant	Naïve	6	7	7 (100)	7 (100)	7 (100)	7 (100)
Mutant	Vehicle	6	9	9 (100)	9 (100)	9 (100)	9 (100)
Mutant	Rapamycin	6	7	7 (100)	6 (85.7)	2 (28.6)	3 (42.9)
Wild type	Naïve	9	6	0 (0)	0 (0)	0 (0)	0 (0)
Mutant	Naïve	9	7	7 (100)	7 (100)	7 (100)	7 (100)
Mutant	Vehicle	9	8	8 (100)	8 (100)	8 (100)	8 (100)
Mutant	Rapamycin	9	7	7 (100)	5 (71.4)	2 (28.6)	1 (14.3)

Percentage of animals is given in parentheses.

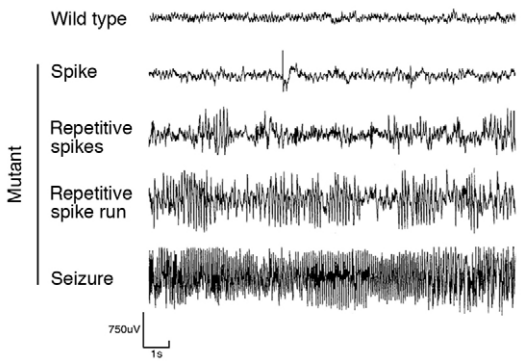

Fig. 4. NS-*Pten* mutant animals show abnormal epileptiform activity. Representative EEG traces from awake, adult mutant mice showing examples of different types of epileptiform activity. All of the mutant mice (*n*=7) analyzed at 6 or 9 weeks of age exhibited isolated interictal spikes, short trains of repetitive spikes lasting less than 5 seconds, repetitive spike runs lasting greater than 5 seconds, and subclinical seizures lasting at least 10 seconds. None of these activities was seen in wild-type animals (*n*=6).

repetitive spikes lasting less than 5 seconds, and long runs of repetitive spikes lasting between 5 and 10 seconds (Fig. 4). Although individual animals varied with respect to the frequency and duration of these EEG patterns, all these types of epileptiform activity were observed in all of the mutants by 6 weeks of age. By 9 weeks of age, these abnormal EEG findings were more frequent than those observed at 6 weeks of age (Fig. 6A).

Rapamycin treatment suppresses mTOR activity and the hypertrophy of cortical Pten-deficient neurons in NS-*Pten* mice

Since hypertrophic Pten mutant cortical neurons demonstrated elevated mTOR activity, we investigated whether treatment with the specific mTOR inhibitor rapamycin could rescue the cellular and molecular abnormalities of mutant mice. Mutant NS-*Pten* mice were treated for 2 weeks with rapamycin or with vehicle (control), and then sacrificed at the end of the treatment to examine mTOR activity in brain sections. We conducted double immunofluorescence experiments using antibodies against phospho-S6, to measure mTOR activity, and NeuN, the general neuronal marker. The levels of phospho-S6 appeared dramatically reduced in the cortical neurons of mutant mice treated with rapamycin compared with vehicle-treated controls, whereas levels of NeuN were similar (Fig. 5A). Quantitative analysis further confirmed that, relative to NeuN, the levels of phospho-S6 were reduced significantly in rapamycin-treated mutants that were examined either immediately after the end of the treatment (6 weeks of age) or 3 weeks later (at 9 weeks of age) (Fig. 5B).

To determine whether rapamycin treatment rescued neuronal hypertrophy, we measured the soma size of cortical layer V pyramidal neurons in vehicle- and rapamycin-treated animals that were sacrificed either immediately after the 2-week treatment (6-week age group) or at 3 weeks after cessation of the treatment (9-week age group). In the animals examined immediately after treatment, we found a modest but significant decrease (~1.2-fold) in the neuronal cell body size in the rapamycin-treated animals (340.7±22.1 μm^2) compared with controls (410.3±5.2 μm^2). However, no significant difference was found in the 9-week old animals that had not been receiving treatment during the previous 3 weeks (rapamycin=414.4±31.5 μm^2; vehicle=448.5±49 μm^2) (Fig. 5C).

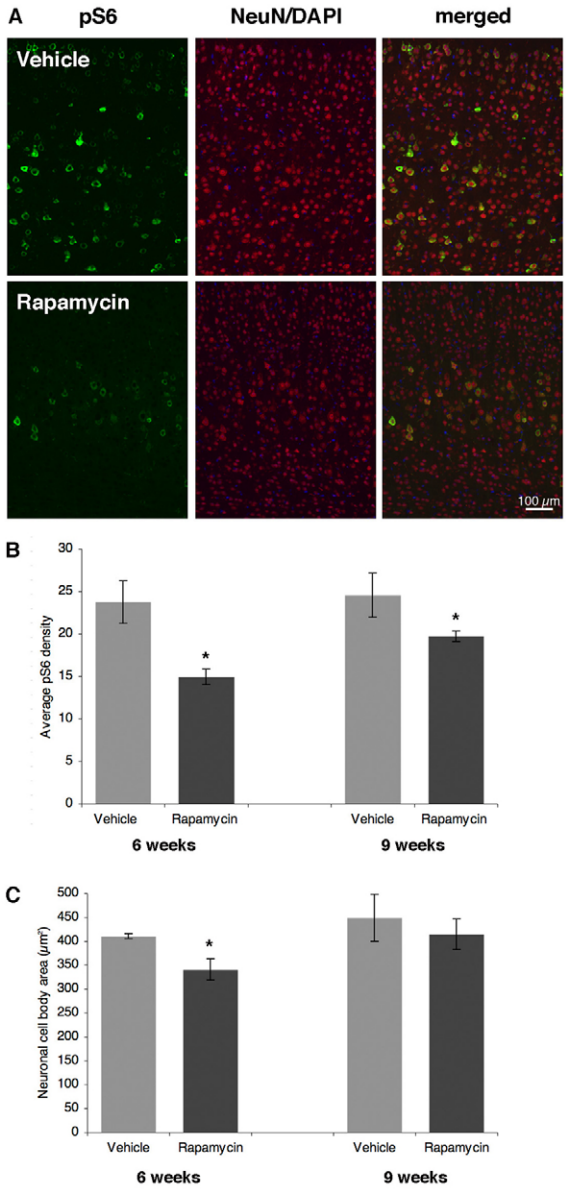

Fig. 5. Rapamycin treatment reduces the phospho-S6 immunoreactivity and hypertrophy of Pten mutant cortical neurons. Four-week-old mutant mice were treated with rapamycin or vehicle for 2 weeks and then processed for immunofluorescence, either immediately (6 weeks of age) or 3 weeks later (9 weeks of age; *n*=5 mice per treatment group). (A) Nine-week-old rapamycin-treated animals (bottom panels) exhibit a marked reduction in phospho-S6 (pS6) immunofluorescence compared with vehicle-treated animals (top panels), whereas expression of the neuronal marker NeuN does not change. (B) Quantification of the fluorescence shows that the level of S6 phosphorylation is reduced in rapamycin-treated animals at 6 weeks of age (*n*=3 mice per treatment group) and that the reduction persists to 3 weeks after cessation of the treatment (9 weeks; *n*=5 mice per treatment group) (*P<0.05). (C) There is a significant decrease in the neuronal soma size in rapamycin-treated animals at 6 weeks of age (*n*=3 mice per treatment group), but not at 9 weeks of age (*n*=4 mice per treatment group) (*P<0.05).

Rapamycin treatment reduces the severity of electrographic abnormalities in NS-*Pten* mice

Having determined that a short-term treatment with rapamycin suppresses, at least in part, the molecular and cellular abnormalities of NS-*Pten* mutant mice, we next determined whether this drug also suppresses the abnormal epileptiform activity observed in these animals. Mutant mice received EEG electrode placement at 3 weeks of age and were then treated with rapamycin or vehicle (control), or were untreated (naïve). Video-EEG recordings were analyzed immediately following treatment (6 weeks of age) and at 3 weeks after treatment was terminated (9 weeks of age). We found that, during the period of video-EEG recording at the 6 week time point, rapamycin-treated mutants spent significantly less time (median=2.9%) in repetitive spikes, repetitive spike runs, or in seizure activity as compared with vehicle-treated (38.4%) or naïve (39.6%) mutants (Fig. 6A). Interestingly, even at three weeks after cessation of treatment, the mutants that had received rapamycin spent significantly less time in epileptiform activity (median=2.8%) than either vehicle-treated (47.0%) or naïve (62.9%) controls.

When different types of EEG abnormalities were analyzed separately, we also found that fewer rapamycin-treated mice displayed all forms of epileptiform activity (Table 1). Whereas 100% of naïve and vehicle-treated mutants exhibited all four types of epileptiform activity by 6 weeks of age, only two of seven (28.6%) rapamycin-treated animals exhibited every type. By 9 weeks, only one of seven rapamycin-treated mutants exhibited electrographic seizures in addition to both short and long trains of repetitive spikes. Isolated interictal spikes, however, were present in all mutant animals, regardless of age or treatment.

Rapamycin treatment also noticeably improved the abnormal awake baseline EEG activity of mutant NS-*Pten* mice (Fig. 6B). Even at three weeks after cessation of treatment, the baseline EEG activity of rapamycin-treated mutants appeared similar to the baseline of wild-type mice. The baseline background activity of naïve and vehicle-treated mutants, however, was unchanged and remained abnormal. These findings may be related to the blockade of seizure activity or could be an effect of the rapamycin itself. However, it appears to be long lasting, even after termination of rapamycin treatment.

DISCUSSION

In this study we characterized NS-*Pten* mutant mice as the first reported genetic animal model for cortical dysplasia. This model does not recapitulate all morphological aspects of the human disease, for example we do not see the dyslamination that is typical of severe cortical dysplasia, or the loss of apical dendrites that occurs in some cytomegalic neurons. However, NS-*Pten* mutant mice recapitulate several key neuropathological features of cortical dysplasia: they exhibit enlarged cortical neurons in which the mTOR kinase is overactive, and spontaneous epileptiform activity that can be detected by EEG. Furthermore, we have demonstrated that treatment with the mTOR inhibitor rapamycin dramatically suppresses the epileptiform activity in NS-*Pten* mutant mice. This antiepileptic effect appears to be long lasting, persisting for at least 3 weeks after cessation of the treatment. Thus, we suggest that NS-*Pten* mice may be useful in the development of new antiepileptic treatments for patients with cortical dysplasia and other mTOR-dependent abnormalities.

As general cortical dysplasia models, NS-*Pten* mutant mice complement the existing collection of genetically modified animals that more specifically model TSC. These latter models include the Eker rat (a heterozygous *Tsc2* mutant) and several transgenic Cre mouse lines that drive conditional *Tsc1* and *Tsc2* knockout deletions in neurons, glial or progenitor cells (reviewed by Holmes and Stafstrom, 2007). Notably, $Tsc1^{GFAP}$ knockout mice, in which the *Tsc1* gene was deleted specifically in mature astrocytes, exhibit seizures similar to NS-*Pten* mice, which improve with rapamycin treatment (Zeng et al., 2008). Similar to our studies, these authors found that early treatment with rapamycin prevented seizures and improved interictal EEG activity, although they found no long-lasting anti-epileptic effect when rapamycin treatment was halted. Our study further supports a role for aberrant mTOR signaling in the generation of seizures, and suggests that mTOR pathway inhibitors are potential therapies for TSC and related disorders.

One major finding of the present studies is that a short period of treatment with rapamycin suppresses the frequency and severity of electrographic seizures in NS-*Pten* mutant mice, indicating that aberrant regulation of the PI3K-mTOR pathway in these mice underlies the epilepsy phenotype. The dramatic effect of rapamycin on the epilepsy phenotype in the NS-*Pten* mutant mice raises the possibility that rapamycin could be developed as a therapy for epilepsy in FCD, HMEG and TSC patients, who are expected to have abnormal activation of PI3K-mTOR signaling in cortical neurons. Interestingly, a reduction of seizure frequency associated with astrocytoma tumor regression and behavioral improvement has been reported in a small group of TSC patients who were treated with the rapamycin analog RAD001 (everolimus) (Franz et al., 2006). Clearly, further clinical investigation of mTOR signaling in epilepsy and an assessment of the efficacy of rapamycin derivatives in TSC, as well as in forms of cortical dysplasia, are necessary. In parallel, further studies in multiple animal models are needed to better assess the utility and the limitations of this intervention strategy.

Although Cre expression in NS-*Pten* mice is driven by the *Gfap* promoter, no Pten mutant astrocytes have been found, indicating that Cre expression occurs only in some neuronal progenitors and not in glial precursors (Backman et al., 2001; Kwon et al., 2001). Thus, we hypothesize that the seizure phenotype observed in NS-*Pten* mutants results primarily from a neuronal dysfunction. However, further studies will be required to evaluate this possibility and to determine whether it originates in cortical, subcortical or hippocampal structures.

Using the same conditional knockout line employed in the present studies, other investigators have reported previously that homozygous *Pten* mutant mice display macrocephaly, behavioral seizures and ataxia (Backman et al., 2001; Kwon et al., 2001). Both of these studies focused on the presence of enlarged neurons in the dentate gyrus and cerebellum, and proposed that *Pten* mutants are good models for Lhermitte-Duclos disease, a human genetic disorder caused by a *PTEN* germline mutation and characterized by cerebellar gangliocytomas. In the present study, we have shifted our attention to the abnormalities in the cerebral cortex, but readily observed the presence of hypertrophic granule neurons in the hippocampus and cerebellum, and the corresponding enlargement of these structures. We also observed the presence of cerebellar-

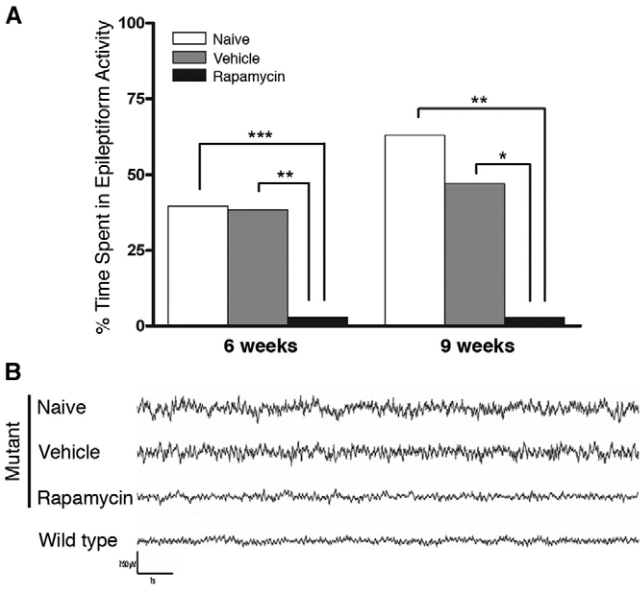

Fig. 6. Rapamycin treatment reduces epileptiform activity in NS-*Pten* mutant mice. (A) The median percent of time that mutant animals spent in repetitive spikes, repetitive spike runs, and/or seizure activity at 6 and 9 weeks of age. Immediately following treatment (6 weeks), rapamycin-treated mutant (n=7) mice spent a significantly reduced amount of time in epileptiform activity compared with vehicle-treated (n=9) or naïve (n=7) animals. Three weeks after treatment termination (9 weeks), epileptiform activity was still significantly reduced for rapamycin-treated animals (n=7) compared with vehicle-treated (n=8) or naïve (n=7) animals. *P<0.05, **P<0.01, ***P<0.001. (B) Representative EEG traces taken during awake baseline activity at 9 weeks of age, illustrating the similarity of the background activity between wild type and rapamycin-treated mutant traces when compared with those seen in naïve and vehicle-treated mutants.

derived ataxia in older mice, as well as increased mortality. We further explored the forebrain phenotype using video-EEG and identified abnormal baseline EEG and epileptiform activity. Thus, our observations are consistent with previous reports, but emphasize different behavioral, neurophysiological and anatomical features that have not previously been analyzed in detail.

Using the neuron-specific enolase (*Nse*) promoter to drive Cre expression, other investigators have described the phenotype of mutant mice in which *Pten* was deleted in mature neuronal populations (Kwon et al., 2006). In addition to macrocephaly and neuronal hypertrophy, these authors reported a behavioral phenotype characterized by sporadic seizures, altered social interaction and inappropriate response to sensory stimuli. Based on these findings, they proposed that *Nse-Pten* mutants are valuable models for autism spectrum disorder (ASD), which is linked to the activation of the PI3K-mTOR pathway. Indeed, a modest degree of comorbidity of ASD with TSC and epilepsy has been reported (Gabis et al., 2005). Although patients with germline *PTEN* mutations do not exhibit seizures, it is interesting to note that a correlation exists between macrocephaly, *PTEN* mutations and autism (Zori et al., 1998; Goffin et al., 2001; Butler et al., 2005). *Nse-Pten* mice also exhibit altered circadian rhythms (Ogawa et al., 2007). These reports provide additional support for the concept that, through modulation of the PI3K-mTOR pathway, Pten activity critically regulates cortical excitability and cognitive function.

We observed a transient reduction in the cell body size of the mutant cortical neurons following a 2-week treatment with rapamycin. These results are also consistent with a previous report (Kwon et al., 2003), in which treatment with the rapamycin analog CCI-779 reduced the cell size of Pten mutant neurons in the dentate gyrus and cerebellum. Unlike the effect on neuronal hypertrophy, we found that a short-term treatment with rapamycin produced a long-lasting effect on suppression of epileptiform activity on the EEG; this effect persisted even at 3 weeks after the cessation of treatment. This leads us to believe that the long-lasting epileptiform suppression by rapamycin treatment is not the result of soma size reduction, but perhaps the result of changes in subcellular structures and, possibly, in downstream molecular targets of mTOR that are involved in synaptic plasticity and membrane excitability. Increasingly, both in vivo and in vitro studies are revealing links between increased mTOR pathway activation and changes in both dendritic and axonal morphology (Jaworski et al., 2005; Kumar et al., 2005; Tavazoie et al., 2005; Kwon et al., 2006). Additionally, links have been made between this pathway and changes in certain ion channels, receptors and the expression of synaptic plasticity (Hou and Klann, 2004; Raab-Graham et al., 2006; Ruegg et al., 2007). Further studies will be required to determine the molecular mechanism underlying the regulation of neuronal network excitability by mTOR. Together with previous studies in animal models, which documented prolonged survival and improved neurological function in association with mTOR inhibition using either rapamycin or its analogues (Kwon et al., 2003; Zeng et al., 2008), our findings raise the hope that a limited modulation of mTOR activity may be sufficient to achieve long-lasting seizure control in some cortical dysplasia and TSC patients, especially those who are currently neither helped by the available pharmacological treatments nor are suitable candidates for epilepsy surgery.

METHODS

Mice

The generation of conditional neuron subset-specific *Pten* (NS-*Pten)* knockout mice (*Gfap-Cre; Pten*$^{loxP/loxP}$) has been described previously (Kwon et al., 2001). The mice were a gift from S. Baker (St Jude Children's Research Hospital, Memphis, TN). In this study we used NS-*Pten*$^{loxP/+}$ (heterozygote) animals for breeding to generate NS-*Pten*$^{+/+}$ (wild type) and NS-*Pten*$^{loxP/loxP}$ (mutants). Animal housing and use were in compliance with the NIH guidelines for the care and use of laboratory animals, and were approved by the institutional animal care committee at Baylor College of Medicine.

Histology, immunohistochemistry and immunofluorescence

Postnatal brains were fixed in 10% neutral buffered formalin (NBF, VWR), embedded in paraffin and 6 μm parasagittal sections were then cut on a microtome. One section from each animal was stained with H&E; adjacent sections were used for immunohistochemistry or immunofluorescence. For experiments using postnatal brain tissue, we performed antigen retrieval in 1 mM citric acid (pH 6) in a steamer for 30 minutes, plus 20 minutes cooling time, for all antibodies except NeuN, which required 1 mM EDTA (pH 8).

Endogenous peroxidase activity was blocked with 1.8% H_2O_2 [in PBS with 0.1% Triton X-100] and the sections were incubated with 10% normal goat or donkey serum (Jackson ImmunoResearch Laboratories) in PBS with 0.1% Triton X-100. For the analysis of cortical layers, embryonic brains were submersion fixed overnight in 4% paraformaldehyde (v/w), cryoprotected in 30% sucrose (v/w) overnight, and 20 µm sections were then cut on a cryostat. Primary antibodies were: Pten (rabbit polyclonal, 1:50, Cell Signaling Technologies, or mouse monoclonal, 1:1600, Cascade Bioscience), NeuN (mouse monoclonal, 1:50, Chemicon), glutamate (rabbit polyclonal, 1:1600, Sigma), phospho-Ser473-Akt (rabbit polyclonal, 1:50, Cell Signaling), GABA (rabbit polyclonal, 1:400, Chemicon), phospho-Ser1108-eIF4G (rabbit polyclonal, 1:50, Cell Signaling), phospho-Ser240/244-S6 (rabbit monoclonal, 1:100, Cell Signaling), Cux1 (rabbit polyclonal, 1:200, Santa Cruz) and foxp2 (goat polyclonal, 1:200, Santa Cruz). All primary antibodies were diluted in PBS with 0.1% Triton X-100 and antibody binding was performed overnight at 4°C. For immunohistochemistry, we used biotin-labeled secondary antibodies raised in goat (1:200, Jackson ImmunoResearch Laboratories) followed by peroxidase-conjugated avidin (Vectastain Elite ABC kit, Vector Laboratories), which was detected by 3,3′-diaminobenzidine (DAB) substrate (Vector Laboratories). Slides were counterstained with Mayer's hematoxylin (VWR) and mounted in Cytoseal 60 (VWR). For immunofluorescence, we used donkey anti-rabbit, anti-mouse or anti-goat secondary antibodies conjugated with Alexa Fluor 488 or 594 (1:1000, Invitrogen). Slides were mounted in Vectashield with DAPI (Vector Laboratories). Fluorescence microscopy was performed using an Olympus BX61 microscope equipped with epifluorescence filters and a Hamamatsu monochrome digital camera, and bright field microscopy was performed using an Olympus BX51 microscope equipped with an Olympus DP70 digital color camera.

Rapamycin treatment

Rapamycin (LC Laboratories) was dissolved in a vehicle solution containing 4% ethanol, 5% polyethylene glycol 400 (Sigma) and 5% Tween 80 (Sigma), essentially as described previously (Eshleman et al., 2002). During the fourth and fifth weeks of life, animals received daily 10 mg/kg intraperitoneal injections, five times per week, of either rapamycin or vehicle. Prior to the 2-week treatment, mice were implanted during postnatal week 3 with EEG electrodes. Video-EEG recordings were collected throughout the 2-week treatment and during the 3-week period following treatment. The mice were then euthanized and the brains were processed as described above.

Electrode implantation

Cortical EEG electrodes were implanted in wild-type and mutant NS-*Pten* mice during postnatal week 3; then, starting at postnatal week 4, the mice were monitored using video-EEG until week 9 when they were euthanized and their brains were processed as described above. Animals were anaesthetized with a ketamine-xylazine-acepromazine mixture (obtained from the Baylor College of Medicine Center for Comparative Medicine) and placed in a stereotaxic frame fitted with a mouse adaptor. Four 0.125 mm diameter stainless steel electrodes (Plastics One) were placed bilaterally over the cortex, two at the anterior and two at the posterior, and a reference was placed anterior to the bregma and a ground was placed in the cervical paraspinous area. Animals were allowed to recover for 4-7 days before video-EEG recording.

EEG acquisition and analysis

After recovery from surgery, a digital video-EEG system (Stellate) was used to record synchronized video-EEGs at an average of twice per week, for 2 to 4 hours per recording. In a subset of animals, recordings lasted for 8 hours per session. Two investigators (A.E.A. and C.N.S.) retrospectively reviewed the traces obtained from the recording sessions. Except for a 20-minute acclimation period, entire video-EEG traces were scored for the presence of isolated spikes, repetitive spike trains, long runs of repetitive spikes, and seizures. Isolated spikes were defined as fast (<200 milliseconds) single events of high amplitude (5× baseline), whereas repetitive spikes included trains of fast spikes and/or spike and slow wave combinations lasting less than 5 seconds. Any repetitive spike and wave activity lasting greater than 5 seconds but less than 10 seconds was classified as a repetitive spike run. Seizures were defined as repetitive spiking activity, or a combination of high-frequency and -amplitude trains of activity, or low frequency, high-amplitude spike and wave discharges that lasted for at least 10 seconds. The associated behavior of the animal was noted during these electrographic events.

We also analyzed the effect of a 2-week vehicle or rapamycin treatment on the EEG activity in mutant animals and compared it to that of naïve mutant animals at 6 and 9 weeks of age. For this part of the study, the video-EEGs were collected and analyzed as described above. In addition, we selected 30-minute samples of EEG traces after 1-hour acclimation in the recording chamber and quantified the amount of time (in seconds) spent in repetitive spikes, repetitive spike runs or seizure activity, and reported this data as the percentage of the total 30-minute (1800-second) observation time. Any activity lasting less than half a second was not counted as epileptiform, hence isolated interictal spikes were eliminated. Investigators who were blinded to the treatment performed this analysis. Data were not of equal variance, and so were analyzed with the Kruskal-Wallis test and the median values were plotted. Post-hoc analysis was accomplished using Dunn's method. These 30-minute epochs were found to be representative of entire recordings when scores from a subset of 9-week EEG recordings (two per treatment group, n=6) were compared with a second 30-minute epoch taken 2-3 hours into the same recording (paired t-test, P=0.37).

Neuronal soma size measurement

For naïve animals, we measured the soma size of pyramidal neurons in cortical layer V in P12 and adult brains from both wild-type and mutant animals (n=3 for each age and genotype). For our measurements, we selected a 1 mm^2 area that was immediately dorsal to the hippocampus on parasagittal sections. We used Pten immunohistochemistry with a hematoxylin counterstain to differentiate Pten-positive pyramidal neurons from Pten-negative neurons in mutant mice, and we measured the Pten-positive pyramidal neurons in wild-type animals using the ImageJ software (NIH). Only cells with a pyramidal-shaped soma and a clear nucleolus were measured. We measured 37±19 (mean±s.d.) Pten-negative neurons and 63±18 Pten-positive neurons in each mutant mouse, and 81±20 Pten-positive neurons in each wild-type mouse.

TRANSLATIONAL IMPACT

Clinical issue

Most cases of intractable childhood epilepsy are caused by malformations of the cerebral cortex known as cortical dysplasia. Currently, progress in understanding and treating cortical dysplasia is hindered by a lack of animal models that recapitulate key features of the disease, such as the presence of abnormal cell types, structural cortical abnormalities and seizures.

The molecular basis of most types of cortical dysplasia is unknown. Recent studies using human brain tissue suggest that a misregulation of the PI3K (phosphoinositide 3-kinase)-Akt-mTOR (mammalian target of rapamycin) signaling pathway might be responsible for the excessive growth of dysplastic cells in this disease. Other studies support the notion that it is the dysplastic cells, or their faulty networks, that cause the seizures. This raises the possibility of using the mTOR inhibitor rapamycin as an antiepileptic treatment for patients with cortical dysplasia.

Results

In this report, the authors characterize a conditional *Pten* knockout mouse as an animal model of cortical dysplasia. The *Pten* gene, which encodes a suppressor of the PI3K-mTOR pathway, was selectively disrupted in a subset of neurons. These mutant mice have several key features seen in cortical dysplasia, such as enlarged cortical neurons with increased mTOR activity, and abnormal electrographic activity with spontaneous seizures. Similar to patients with focal cortical dysplasia (FCD), the time of onset and the severity of the seizures varied. However, by 6 weeks of age, all mutant mice exhibited seizures and benefited from short-term treatment with the mTOR inhibitor rapamycin. This drug reduced the mTOR activity in the enlarged neurons, transiently reduced the size of the enlarged neurons, and strongly suppressed the severity and the duration of the epileptiform activity.

Implications and future directions

This paper presents a conditional *Pten* knockout mouse that is a novel model of cortical dysplasia. Furthermore, treatment of these mice with the drug rapamycin suppresses seizures. Previous studies in other seizure-prone mouse models have also demonstrated that treatment using either rapamycin or its analogues results in prolonged survival and improved neurological function. Together, these findings suggest that a limited modulation of mTOR activity may be sufficient to achieve long-lasting seizure control in some cortical dysplasia patients, especially those who are currently neither helped by available pharmacological treatments nor are suitable candidates for epilepsy surgery.

doi:10.1242/dmm.003558

Data are presented as soma size in μm^2±s.e.m. and are analyzed using ANOVA and Tukey's HSD.

For rapamycin- and vehicle-treated animals, the soma size of Pten-negative pyramidal neurons in the layer V cortex was measured, as described above, in animals that were either euthanized directly after the 2-week treatment (n=3, vehicle or rapamycin) or in the group that was followed by EEG until 9 weeks of age (n=4, vehicle or rapamycin). We measured 36±13 (mean±s.d.) Pten-negative neurons in each animal and the data were analyzed using the Student's t-test.

Analysis of fluorescence intensity

We performed Pten and phospho-S6 double immunofluorescence and compared the phospho-S6 signal intensity in the cortical layer V Pten-positive neurons with the Pten-negative neurons in sections obtained from 9-week mutant mice (n=3) using the ImageJ software (NIH). The phospho-S6 pixel values in Pten-negative neurons were expressed in each animal as the fold change compared with the phospho-S6 pixel values in Pten-positive neurons. Data were analyzed using one sample t-test. Using a modified protocol, we also analyzed the phospho-S6 immunofluorescence intensity in vehicle- and rapamycin-treated animals, directly after the 2-week treatment protocol (n=3 for each of the vehicle- or rapamycin-treated animals) or at 9 weeks of age (n=5 for each treatment group), using NeuN and DAPI immunofluorescence to define the neuronal cytosol. For each animal, three non-overlapping adjacent fields of the neocortex dorsal to the hippocampus were selected, including layers I-VI, and three images (phospho-S6 in green, NeuN in red and DAPI in blue) were collected using the same camera settings. Using a Matlab script developed by T. J. Vadakkan, we created a threshold for all of the NeuN images to include only positive neurons. Since the localization of phospho-S6 is cytoplasmic, we excluded the DAPI-stained nuclei from the analysis. We then compared the phospho-S6 signal with the NeuN signal (control) in the cytoplasm. Data were analyzed using two-way ANOVA.

ACKNOWLEDGEMENTS

We thank S. Baker for the gift of NS-*Pten* mice; B. A. Antalffy, D. Parghi and the Mental Retardation and Developmental Disabilities Research Center at Baylor College of Medicine for help with tissue processing; S. Willis and F. Vanegas-Roman for assistance with EEG electrode implants; T. J. Vadakkan for programming the fluorescence analysis; R. Azevedo for the use of the Olympus BX-61 microscope and advice on statistical analysis; and J. Swann for critical reading of the manuscript. This work was supported by a 2004 Research Award and a 2007 Challenge Award from the Citizens United for Research in Epilepsy (CURE) (to G.D.), NIH/NINDS R01 NS042616 (to G.D.), a pre-doctoral fellowship from the American Epilepsy Foundation (to C.N.S.), a postdoctoral fellowship from the American Epilepsy Foundation (to J.N.L.), NIH/NINDS F32 NS056664 (to J.N.L.) and NIH/NINDS R01 NS049427 (to A.E.A.). Deposited in PMC for release after 12 months.

COMPETING INTERESTS

The authors declare no competing financial interests.

AUTHOR CONTRIBUTIONS

M.C.L. and C.N.S. contributed equally to this work. M.C.L. and C.N.S. designed some of the experiments, performed the experiments, analyzed the data, wrote parts of the manuscript and edited the manuscript. J.N.L. performed some experiments and edited the manuscript. A.E.A. designed some of the experiments, analyzed the data and edited the manuscript. G.D. conceived the study, designed some of the experiments and wrote the manuscript.

Received 4 December 2008; Accepted 9 March 2009.

REFERENCES

Backman, S. A., Stambolic, V., Suzuki, A., Haight, J., Elia, A., Pretorius, J., Tsao, M. S., Shannon, P., Bolon, B., Ivy, G. O. et al. (2001). Deletion of Pten in mouse brain causes seizures, ataxia and defects in soma size resembling Lhermitte-Duclos disease. *Nat. Genet.* **29**, 396-403.

Backman, S., Stambolic, V. and Mak, T. (2002). PTEN function in mammalian cell size regulation. *Curr. Opin. Neurobiol.* **12**, 516-522.

Baybis, M., Yu, J., Lee, A., Golden, J. A., Weiner, H., McKhann, G., 2nd, Aronica, E. and Crino, P. B. (2004). mTOR cascade activation distinguishes tubers from focal cortical dysplasia. *Ann. Neurol.* **56**, 478-487.

Butler, M. G., Dasouki, M. J., Zhou, X. P., Talebizadeh, Z., Brown, M., Takahashi, T. N., Miles, J. H., Wang, C. H., Stratton, R., Pilarski, R. et al. (2005). Subset of individuals with autism spectrum disorders and extreme macrocephaly associated with germline PTEN tumour suppressor gene mutations. *J. Med. Genet.* **42**, 318-321.

Cepeda, C., Andre, V. M., Levine, M. S., Salamon, N., Miyata, H., Vinters, H. V. and Mathern, G. W. (2006). Epileptogenesis in pediatric cortical dysplasia: the dysmature cerebral developmental hypothesis. *Epilepsy Behav.* **9**, 219-235.

Chow, L. M. and Baker, S. J. (2006). PTEN function in normal and neoplastic growth. *Cancer Lett.* **241**, 184-196.

Eng, C. (2003). PTEN: one gene, many syndromes. *Hum. Mutat.* **22**, 183-198.

Eshleman, J. S., Carlson, B. L., Mladek, A. C., Kastner, B. D., Shide, K. L. and Sarkaria, J. N. (2002). Inhibition of the mammalian target of rapamycin sensitizes U87 xenografts to fractionated radiation therapy. *Cancer Res.* **62**, 7291-7297.

European Chromosome 16 Tuberous Sclerosis Consortium (1993). Identification and characterization of the tuberous sclerosis gene on chromosome 16. *Cell* **75**, 1305-1315.

Franz, D. N., Leonard, J., Tudor, C., Chuck, G., Care, M., Sethuraman, G., Dinopoulos, A., Thomas, G. and Crone, K. R. (2006). Rapamycin causes regression of astrocytomas in tuberous sclerosis complex. *Ann. Neurol.* **59**, 490-498.

Fraser, M. M., Zhu, X., Kwon, C. H., Uhlmann, E. J., Gutmann, D. H. and Baker, S. J. (2004). Pten loss causes hypertrophy and increased proliferation of astrocytes *in vivo*. *Cancer Res.* **64**, 7773-7779.

Gabis, L., Pomeroy, J. and Andriola, M. R. (2005). Autism and epilepsy: cause, consequence, comorbidity, or coincidence? *Epilepsy Behav.* **7**, 652-656.

Goffin, A., Hoefsloot, L. H., Bosgoed, E., Swillen, A. and Fryns, J. P. (2001). PTEN mutation in a family with Cowden syndrome and autism. *Am. J. Med. Genet.* **105**, 521-524.

Harris, T. E. and Lawrence, J. C., Jr (2003). TOR signaling. *Sci STKE* 2003, re15.

Holmes, G. L. and Stafstrom, C. E. (2007). Tuberous sclerosis complex and epilepsy: recent developments and future challenges. *Epilepsia* **48**, 617-630.

Hou, L. and Klann, E. (2004). Activation of the phosphoinositide 3-kinase-Akt-mammalian target of rapamycin signaling pathway is required for metabotropic glutamate receptor-dependent long-term depression. *J. Neurosci.* **24**, 6352-6361.

Jaworski, J., Spangler, S., Seeburg, D. P., Hoogenraad, C. C. and Sheng, M. (2005). Control of dendritic arborization by the phosphoinositide-3′-kinase-Akt-mammalian target of rapamycin pathway. *J. Neurosci.* **25**, 11300-11312.

Kumar, V., Zhang, M. X., Swank, M. W., Kunz, J. and Wu, G. Y. (2005). Regulation of dendritic morphogenesis by Ras-PI3K-Akt-mTOR and Ras-MAPK signaling pathways. *J. Neurosci.* **25**, 11288-11299.

Kwon, C. H., Zhu, X., Zhang, J., Knoop, L. L., Tharp, R., Smeyne, R. J., Eberhart, C. G., Burger, P. C. and Baker, S. J. (2001). Pten regulates neuronal soma size: a mouse model of Lhermitte-Duclos disease. *Nat. Genet.* **29**, 404-411.

Kwon, C. H., Zhu, X., Zhang, J. and Baker, S. J. (2003). mTor is required for hypertrophy of Pten-deficient neuronal soma *in vivo*. *Proc. Natl. Acad. Sci. USA* **100**, 12923-12928.

Kwon, C. H., Luikart, B. W., Powell, C. M., Zhou, J., Matheny, S. A., Zhang, W., Li, Y., Baker, S. J. and Parada, L. F. (2006). Pten regulates neuronal arborization and social interaction in mice. *Neuron* **50**, 377-388.

Leevers, S. J., Vanhaesebroeck, B. and Waterfield, M. D. (1999). Signalling through phosphoinositide 3-kinases: the lipids take centre stage. *Curr. Opin. Cell Biol.* **11**, 219-225.

Li, J., Yen, C., Liaw, D., Podsypanina, K., Bose, S., Wang, S. I., Puc, J., Miliaresis, C., Rodgers, L., McCombie, R. et al. (1997). PTEN, a putative protein tyrosine phosphatase gene mutated in human brain, breast, and prostate cancer. *Science* **275**, 1943-1947.

Ljungberg, M. C., Bhattacharjee, M. B., Lu, Y., Armstrong, D. L., Yoshor, D., Swann, J. W., Sheldon, M. and D'Arcangelo, G. (2006). Activation of mammalian target of rapamycin in cytomegalic neurons of human cortical dysplasia. *Ann. Neurol.* **60**, 420-429.

Maehama, T. and Dixon, J. E. (1998). The tumor suppressor, PTEN/MMAC1, dephosphorylates the lipid second messenger, phosphatidylinositol 3,4,5-trisphosphate. *J. Biol. Chem.* **273**, 13375-13378.

Miyata, H., Chiang, A. C. and Vinters, H. V. (2004). Insulin signaling pathways in cortical dysplasia and TSC-tubers: tissue microarray analysis. *Ann. Neurol.* **56**, 510-519.

Ogawa, S., Kwon, C. H., Zhou, J., Koovakkattu, D., Parada, L. F. and Sinton, C. M. (2007). A seizure-prone phenotype is associated with altered free-running rhythm in Pten mutant mice. *Brain Res.* **1168**, 112-123.

Podsypanina, K., Ellenson, L. H., Nemes, A., Gu, J., Tamura, M., Yamada, K. M., Cordon-Cardo, C., Catoretti, G., Fisher, P. E. and Parsons, R. (1999). Mutation of Pten/Mmac1 in mice causes neoplasia in multiple organ systems. *Proc. Natl. Acad. Sci. USA* **96**, 1563-1568.

Raab-Graham, K. F., Haddick, P. C., Jan, Y. N. and Jan, L. Y. (2006). Activity- and mTOR-dependent suppression of Kv1.1 channel mRNA translation in dendrites. *Science* **314**, 144-148.

Ruegg, S., Baybis, M., Juul, H., Dichter, M. and Crino, P. B. (2007). Effects of rapamycin on gene expression, morphology, and electrophysiological properties of rat hippocampal neurons. *Epilepsy Res.* **77**, 85-92.

Sarbassov, D. D., Guertin, D. A., Ali, S. M. and Sabatini, D. M. (2005). Phosphorylation and regulation of Akt/PKB by the rictor-mTOR complex. *Science* **307**, 1098-1101.

Suzuki, A., de la Pompa, J. L., Stambolic, V., Elia, A. J., Sasaki, T., del Barco Barrantes, I., Ho, A., Wakeham, A., Itie, A., Khoo, W. et al. (1998). High cancer susceptibility and embryonic lethality associated with mutation of the PTEN tumor suppressor gene in mice. *Curr. Biol.* **8**, 1169-1178.

Tavazoie, S. F., Alvarez, V. A., Ridenour, D. A., Kwiatkowski, D. J. and Sabatini, B. L. (2005). Regulation of neuronal morphology and function by the tumor suppressors Tsc1 and Tsc2. *Nat. Neurosci.* **8**, 1727-1734.

van Slegtenhorst, M., de Hoogt, R., Hermans, C., Nellist, M., Janssen, B., Verhoef, S., Lindhout, D., van den Ouweland, A., Halley, D., Young, J. et al. (1997). Identification of the tuberous sclerosis gene TSC1 on chromosome 9q34. *Science* **277**, 805-808.

Vinters, H. V., Park, S. H., Johnson, M. W., Mischel, P. S., Catania, M. and Kerfoot, C. (1999). Cortical dysplasia, genetic abnormalities and neurocutaneous syndromes. *Dev. Neurosci.* **21**, 248-259.

Zeng, L. H., Xu, L., Gutman, D. H. and Wong, M. (2008). Rapamycin prevents epilepsy in a mouse model of Tuberous Sclerosis Complex. *Ann. Neurol.* **63**, 444-453.

Zori, R. T., Marsh, D. J., Graham, G. E., Marliss, E. B. and Eng, C. (1998). Germline PTEN mutation in a family with Cowden syndrome and Bannayan-Riley-Ruvalcaba syndrome. *Am. J. Med. Genet.* **80**, 399-402.